

Contents lists available at ScienceDirect

Polymer

journal homepage: http://www.elsevier.com/locate/polymer





Damage detection through Förster Resonance Energy Transfer in mechanoresponsive polymer nanocomposites

Meng Wang ^a, Alexandra Schwindt ^b, Kedi Wu ^c, Ying Qin ^c, Allison Kwan ^b, Sefaattin Tongay ^c, Matthew D. Green ^{b,*}

- ^a School of Molecular Sciences, Arizona State University, Tempe, AZ, 85281, USA
- b Chemical Engineering, School for Engineering of Matter, Transport and Energy, Arizona State University, Tempe, AZ, 85281, USA
- c Materials Science and Engineering, School for Engineering of Matter, Transport and Energy, Arizona State University, Tempe, AZ, 85281, USA

ARTICLE INFO

Keywords: Nanocomposite Stimuli-responsive nanocomposite Mechanoresponsive nanocomposite

ABSTRACT

Polymer nanocomposites offer design solutions to control and tune optical, conductive, topological, and thermomechanical properties of advanced and multifunctional materials. Because of their ubiquitous nature, methodologies to diagnose failure or structural changes in the nanocomposites are of significant interest. Herein, we report a nanocomposite system loaded with quantum dots and coumarin-modified carbon nanotubes that transduce mechanical force into fluorescence at a strain, for the first time, as low as 7.5%. Our comprehensive studies detail the optical, morphological, and thermomechanical properties of these nanocomposites to establish the fundamental reason behind the activation of fluorescence. Our results indicate that bare carbon nanotubes can irreversibly quench the fluorescence from quantum dots and that the coumarin-modified carbon nanotubes mitigate the quenching through Förster Resonance Energy Transfer. Next, the application of force to the sample changes the quantum dot-carbon nanotube spacing as well as the carbon nanotube morphology to activate fluorescence in the nanocomposite. Overall, this force activation of fluorescence can serve as a general strategy for the development of a new class of mechano-responsive nanocomposites that impart polymeric materials with desirable functionalities including damage sensing and mechanical strength.

1. Introduction

The ability to understand and predict the response of polymers, polymer resins, and polymer composites to mechanical stress has been of interest to the scientific community for over a century [1]. Shortly after Staudinger's hypothesis of the existence of high molecular weight molecules, he observed reductions in molecular weight caused by mechanical stress [2,3]. Over time, a number of innovative strategies to probe the macroscopic and molecular level responses to mechanical stress have been utilized, including fluorescent indicators [4,5], radical generators [4,5], biased reaction pathways [6], moieties that induce changes in pH [7], dyes that change color [8], acid generators [9], groups that release small molecules [10], and cation generators [11].

Some of these efforts led to the creation of a branch of materials science and engineering that study mechanochemical transduction to activate luminescence [12]. This characteristic is typically based on the formation of nanoscale aggregates of dyes in a polymeric matrix, which leads to a change in the material's optical properties [13]. This effect can

be achieved by physically blending dyes into a host polymer, or covalently attaching them, and can result in reversible on/off activation [14, 15] as well as multi-color responses [16–21]. For example, previously it was reported that a color change could be elicited upon plastic deformation within linear low-density polyethylene (LLDPE) films containing small amounts of cyano-oligo (p-phenylene vinylene) [22]. Similarly, aggregation-induced emission (AIE) is a photophysical phenomenon associated with chromophore aggregation [23]. In the AIE process, non-emissive luminogens are triggered to emit by the formation of aggregates. Photophysical properties of chromophore-containing polymers can also be changed by breaking covalent bonds using mechanical force [24]. Sottos et al. first reported a mechano-active polymer in which spiropyran groups were covalently introduced to bridge between adjacent polymer chains as a "mechanophore" [8]. Upon application of a tensile force, the spiropyran mechanophore undergoes a reversible ring opening reaction and, as a result, the polymer turned a reddish color. Others have placed the spiropyran group into the polymer backbone to improve sensitivity and improve network characteristics [25]. To

E-mail address: mdgreen8@asu.edu (M.D. Green).

^{*} Corresponding author.

facilitate mechanochemical transduction within nanocomposites, mechanophores have been used as a linker between an epoxy matrix and a silk fiber additive; the emission wavelength shift and fluorescence lifetime variations were monitored, which correlated to the applied stress at the silk-epoxy interface [26]. Among all of these strategies, a common feature is that they require the synthesis of polymers with a mechano-responsive moiety, which increases the cost and difficulty of fabricating the material system.

A growing number of investigations use nanoparticles and the nanoparticle-matrix interface to introduce mechanochemical transduction. Polymer nanocomposites are used widely, and the general premise of composites is that additives (big and small) introduce strength and/or functionality to the composite [27]. The size scale of the additive continues to push smaller and smaller in order to introduce and harness new phenomena in the composite [28]. Easy and early detection of emergent (microscopic) damage in fiber-reinforced composite materials is highly desirable. For example, the 'bleeding' mechanism indicates composite failure when a UV fluorescent dye leaks from fractured hollow fibers into damage sites [29]. Others have studied failure in glass-reinforced composites by placing a fluorescent protein at the fiber-matrix interface [30]. By tracking the force-induced vellow light fluorescence caused by the unfolding of the protein, researchers were able to report micron-scale damage, such as fiber fractures and fiber-matrix debonding. The thermal characteristics of the additives can also be utilized; for example, adding boron nitride (which has a high thermal conductivity) to epoxy networks facilitated thermal tracking of composite failure via infrared thermal imaging [31]. Likewise, the electrical resistance of graphene-reinforced epoxy networks increased linearly with elongation and followed an apparent higher-order polynomial relationship with stress [32]. These reports highlight recent efforts to use nano-additives to impart multiple functionalities, one of which is damage detection. Two consistent desires are to decouple composite performance (thermomechanical performance, conductivity, etc.) from diagnostic capability as well as to improve the diagnostic sensitivity (current art requires strains of ~100% to activate diagnostic functions).

In this work, a mechano-responsive epoxy-based composite material was designed based on the fluorescence quenching pair of dye-modified carbon nanotubes (mCNTs) and quantum dots (QDs). Spectral overlap between the emission of the donor and the absorbance of the acceptor is required for fluorescence quenching to occur. Therefore, CdSeS/ZnS alloyed QDs were selected as the quenching pair acceptor. Then, a fluorescent dye, 7-amino-4-methylcoumarin, was conjugated to the surface of CNTs to serve as the donor. The mCNTs and QDs distributed uniformly into the thermoset with the help of ultrasonication. The quenching pair was designed to enable force activation of fluorescence properties. Pronounced changes in fluorescence emerge following plastic deformation, indicating that these polymeric materials are able to transduce mechanical force into fluorescence. Finally, the mechanical stimuli induced aggregation of the mCNTs, which was confirmed using

2. Experimental section

2.1. Materials

Acid modified CNTs were obtained from NanoAmor. N,N-Dimethylformamide (DMF, 99.5%), dicyclohexylcarbodiimide (DCC, 99%), Bisphenol A diglycidyl ether (BADGE, 99%), CdSeS/ZnS alloyed quantum dots (λ em 490 nm, 6 nm diameter, 1 mg/mL in H₂O), and 7-amino-4-methylcoumarin (99%) were obtained from Sigma-Aldrich and used without further purification. Jeffamine T3000 (97%), a trifunctional polyetheramine with a molecular weight of 3000 g/mol, was graciously provided by Huntsman International, LLC. Toluene was obtained from Fisher Scientific and passed through an MBraun solvent purification system prior to use. Isopropyl alcohol (IPA) was obtained

from Fisher Scientific.

2.2. Modification of CNTs

As an example, 1.0 g of acid-modified CNTs (e.g., -COOH modified CNTs) was dispersed in 20 mL of DMF under ultrasonic irradiation (150 W, 23 °C) for 30 min. Then, 0.2 g of 7-amino-4-methylcoumarin and 0.5 g of DCC were added to the solution. The reaction was performed at 80 °C with magnetic stirring for 12 h. Most of the solvent was removed using vacuum filtration, and the filter cake was washed with DMF, toluene, and IPA under ultrasonic irradiation (3 times each for 30 min). The combination of solvent washes and sonication removed unreacted dye and the DCC coupling reaction byproduct. The purified dyemodified CNTs (mCNTs) were placed into a vacuum oven at 80 °C, at full vacuum for 8 h to remove any residual solvent.

2.3. Preparation of mCNT composites

As an example, 12.6 g of BADGE was heated at 50 °C, once it melted 17 g of Jeffamine T3000 was added with magnetic stirring. The mixture was stirred until it became homogeneous. Then, mCNTs were added at the desired concentration from a dispersion in DMF. Altogether, <0.5 mL of the mCNT dispersion was added for $\sim\!30$ g of resin (i.e., <1.5 wt% DMF). The mixture was stirred under ultrasonic irradiation for 30 min. Then, the mixture was stirred again and put in a vacuum oven at 80 °C for 4 h. Finally, the temperature was raised to 120 °C for 4 h. These curing conditions mimic common epoxy resin curing conditions, including our previous work [33], and allow for a precure at lower temperatures followed by a high temperature cure to drive the reaction to complete conversion.

2.4. Preparation of QDs composites epoxy

As an example, 12.6 g of BADGE was heated at 50 $^{\circ}\text{C}$, once it melted 17 g of Jeffamine T3000 was added to the system. The mixture was stirred until it became homogeneous. Then, the quantum dots were added (0.1 mL of the 1 mg/mL aqueous solution per 10 g epoxy). For this case, this amounts to 0.12 mL of solvent for $\sim\!30$ g of resin. The sample was kept under vacuum at 60 $^{\circ}\text{C}$ for 12 h to remove the solvent. The mixture was stirred until uniform and then sonicated for 30 min. The mixture was stirred and then put in a vacuum oven at 80 $^{\circ}\text{C}$ for 4 h and then the temperature was raised to 120 $^{\circ}\text{C}$ for 4 h.

2.5. Preparation of mCNT/QDs composites epoxy

As an example, 12.6 g of BADGE was heated at 50 °C, once it melted 17 g of Jeffamine T3000 was added. The mixture was stirred until it became homogeneous. Then, 0.25 wt% mCNTs were added with several drops of DMF. Next, 0.1 mL of the 1 mg/mL aqueous QDs solution per 10 g epoxy was added. Altogether, this amounts to <0.5 mL of solvent for ~30 g of resin. The sample was kept under vacuum at 60 °C for 12 h to remove the solvent. The mixture was sonicated for 30 min, stirred, and then put in a vacuum oven at 80 °C for 4 h followed by an additional 4 h at 120 °C.

2.6. Characterization

Tensile testing of the composites was performed with an Instron E3000 instrument, the limit of strain was set to be 5 cm and the tensile test was performed at a strain rate of 0.5 mm/min. Steady-state fluorescence emission and excitation spectra of CNT, coumarin, mCNT, and QD solutions in DMF were measured on a Nanolog fluorometer (Horiba Jobin Yvon) using a quartz cuvette with a 10 mm path length and corrected for the wavelength dependence of the detection system response. Diffuse reflectance Fourier-transform infrared spectroscopy (DRIFT) was performed on a Nicolet iS50 FTIR spectrometer with a DTGS KBR

detector, 100 scans were averaged per spectrum and baseline corrections were performed. Photoluminescence (PL) measurements were performed using a Renishaw InVia spectroscopy system in backscattering configuration with a $40 \times$ objective using a UV laser source at a wavelength of 325 nm. The laser was focused onto the sample with a spot diameter of 0.5 µm. Fluorescence microscopy of solid nanocomposite samples was performed with Biotek Cytation 5 image reader under manual mode. The LED intensity was consistently set to 300 (scale of 0–1000) and the exposure time was kept constant for all the samples. The samples were placed on a petri dish and imaged. All samples subjected to strain were either broken in the Instron and transported directly to the microscope or strained to a pre-specified strain value (e. g., those in Fig. 5) and then transported directly to the microscope. The time from tensile testing to imaging was <30 min. TEM samples were prepared with a Leica EM FC 7 cryo-ultramicrotome; samples were cut at $-100~^{\circ}\text{C}$ at a cutting speed of 0.8 mm/s and a 75 nm feed. TEM was performed with JEOL ARM200F operating at 120 kV.

3. Results and discussion

Coumarin-modified CNTs were prepared to serve as a fluorescent quencher and form a Förster Resonance Energy Transfer (FRET) pair with the QDs. The CNTs were modified with 7-amino-4-methylcoumarin providing a blue emission wavelength of λ_{em} 460 nm. The CdSeS/ZnS alloyed QDs possess an excitation wavelength at λ_{ex} 450 nm together with green fluorescence at λ_{em} 525 nm. Together, the fluorescent characteristics of the coumarin dye and the QDs motivate the selection of the pair. First, acid-modified multi-walled CNTs were sonicated in DMF for 30 min to disperse the CNTs in the solution. Then, 7-amino-4-methyl-coumarin and DCC were added and the solution was heated to 80 °C for 24 h (Fig. 1a), which is an adapted protocol from the literature [34]. The mCNTs were then purified of unreacted dye and the reaction byproducts and subjected to further characterization.

Fourier-transform infrared (FTIR) spectroscopy and fluorescence spectroscopy were used to characterize the presence of the fluorescent dye on the CNTs. Fig. 1b shows the infrared transmittance spectra for the fluorescent dye, the acid-modified CNTs, and the dye-modified CNTs.

Distinct changes in the spectra are observed following the conjugation of the dye to the CNTs with several unique absorbance bands appearing that are attributed to the attachment of the dye onto the CNT. Specifically, the amide N–H bond appears at 1503 cm⁻¹ and the R–NH–CO-R' amide bond appears at 1572 cm⁻¹, respectively. The ester bond from the coumarin ring results in an absorbance peak at 1014 cm⁻¹ and 1149 cm⁻¹. Additionally, there are singlet peaks at 483 cm⁻¹, 659 cm⁻¹ and 745 cm⁻¹ indicating a tri-functional benzene ring (e.g., the coumarin aromatic ring). The amide bond appearance validated that coumarin dye was modified onto the surface of CNTs, as it could also be physically adsorbed to the surface of CNTs due to π - π stacking.

Fluorescence spectroscopy was used to measure the fluorescence properties of the CNTs, dye, and dye-modified CNTs separately as well. Excitation/emission spectra for the CNTs, the fluorescent dye, and the dye-modified CNTs, as well as an overlay plot with the emission spectrum from each of the three samples are shown in Fig. 1c–f. The fluorescence of dye-modified CNTs samples show combined fluorescence properties of the CNTs and the dye. Moreover, the fluorescence intensity increases in the order of CNTs < dye-modified CNTs < dye. Importantly, the dye-modified CNTs display an order of magnitude increase in fluorescence intensity after the dye is conjugated.

Next, the fluorescent additives were added to the epoxy resins and cured. Briefly, bisphenol A diglycidyl ether (BADGE) was melted at 50 $^{\circ}$ C and Jeffamine T3000 was added. Next, the mCNTs were added as a dispersion in DMF and 0.1 mL of the aqueous QDs solution was added and stirred (altogether, <0.5 mL of solvent for ~30 g of resin). The solvent was driven off under vacuum at 60 $^{\circ}$ C and then the resin was cured using a two step cure process to produce a thermoset (Scheme 1). BADGE/Jeffamine composites loaded with multi-walled CNTs have been previously reported in the literature, and have shown to make elastomeric, amorphous nanocomposites [33].

The fluorescence quenching phenomenon was observed via photoluminescence (PL) measurements for cured composites containing mCNTs, QDs, or both QDs and mCNTs (Fig. 2a). As expected, the epoxy sample with mCNTs displayed a strong blue fluorescence around 425 nm, whereas the epoxy sample with QDs displayed green fluorescence at 525 nm. It is important to observe that the fluorescence intensity of the

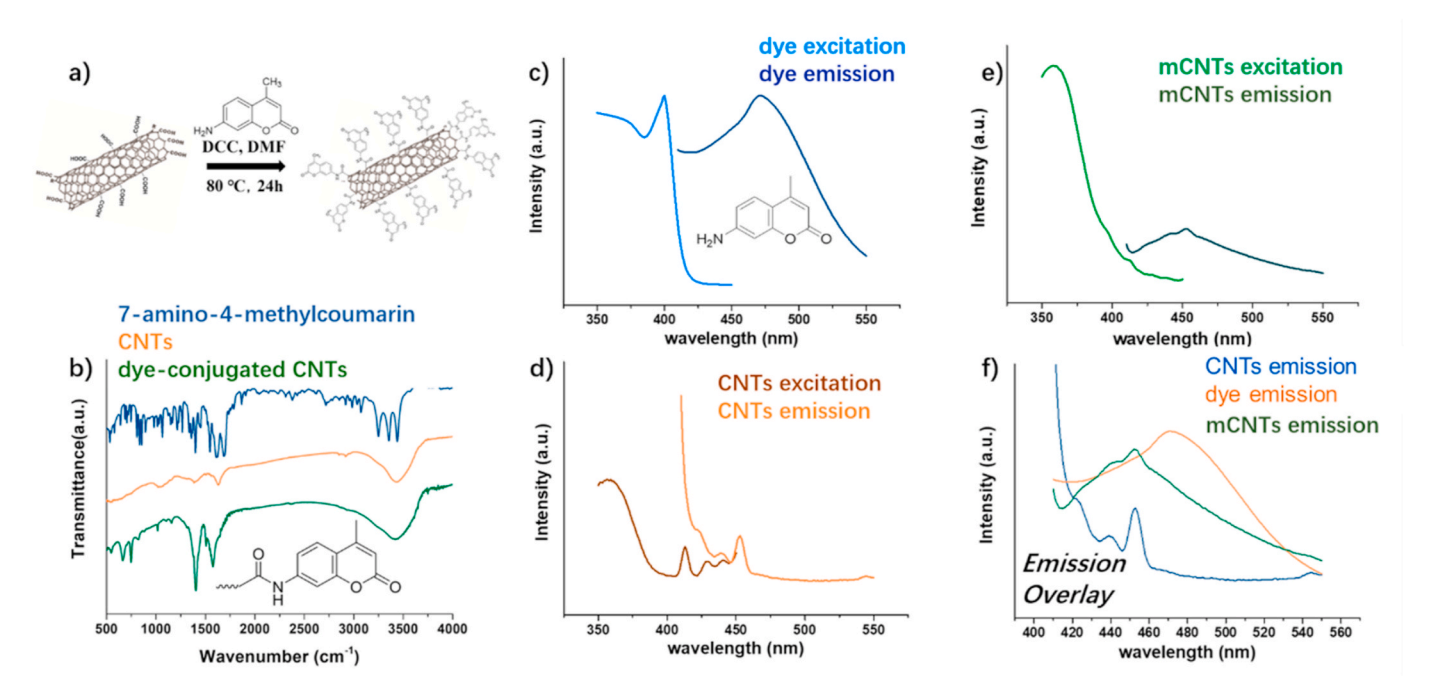
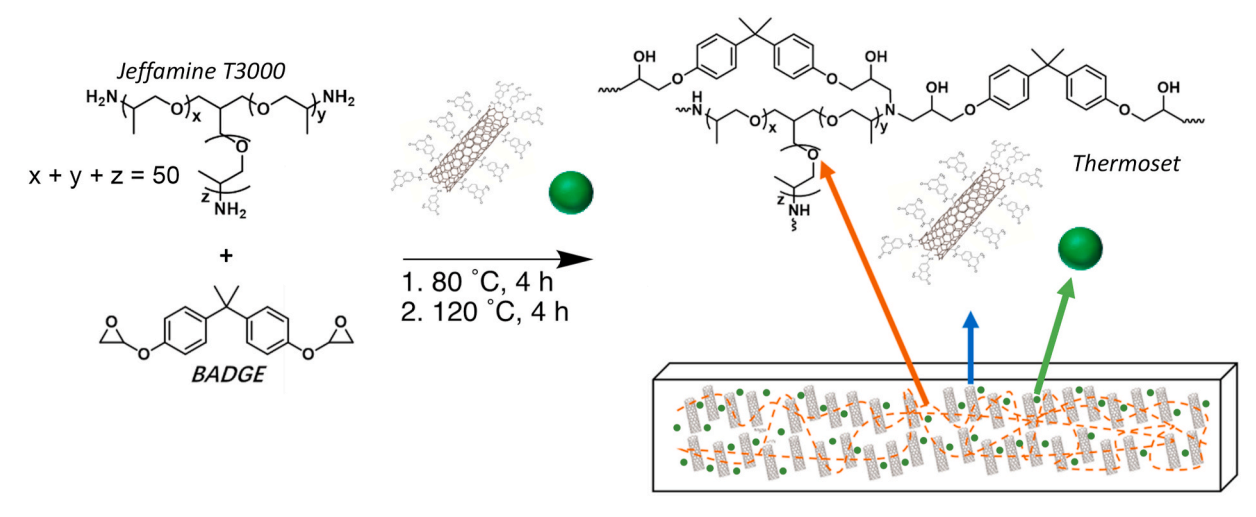


Fig. 1. a) Schematic detailing the procedure used to covalently attach 7-amino-4-methylcoumarin to acid-modified CNTs, b) FTIR spectra of (top) 7-amino-4-methylcoumarin, (middle) acid-modified multi-walled CNTs, and (bottom) dye-modified CNTs. Fluorescence spectroscopy data for: c) the 7-amino-4-methylcoumarin fluorescent dye, d) the acid-modified multi-walled CNTs, e) the dye-modified CNTs, and f) an overlay of fluorescent emission for all three samples.



Scheme 1. Synthesis scheme to prepare elastomeric nanocomposites loaded with dye-modified CNTs and QDs.

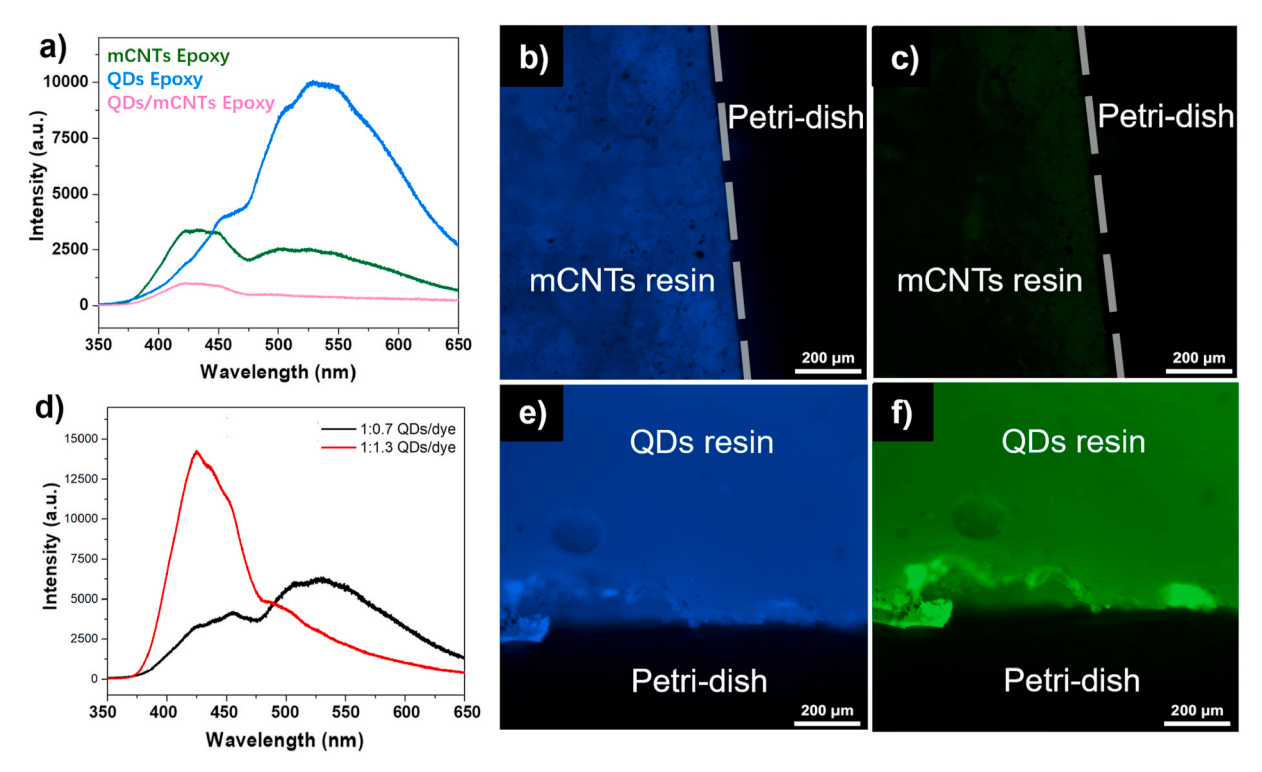


Fig. 2. a) Photoluminescence (PL) intensities for cured composites containing green) mCNTs, blue) QDs, or pink) both QDs and mCNTs– excitation wavelength: 325 nm. b,c) Fluorescence microscopy of composites containing mCNTs; the panels show b) excitation wavelength: 377 nm and emission wavelength: 447 nm, and c) excitation wavelength: 469 nm and emission wavelength: 525 nm. d) Fluorescence emission intensities for a cured composite containing black) dye and an excess amount of QDs, and red) QDs and an excess amount of dye. e,f) Fluorescence microscopy of composites containing QDs. The panels show e) excitation wavelength: 377 nm and emission wavelength: 447 nm, and f) excitation wavelength: 469 nm and emission wavelength: 525 nm. In b, c, e, and f the QD concentration is 0.005 wt % and the mCNT concentration is 0.25 wt%. (For interpretation of the references to color in this figure legend, the reader is referred to the Web version of this article.)

composite with both mCNTs and QDs dramatically decreased compared to composites with either QDs or mCNTs. Next, the coumarin dye ($\lambda_{ex} = 450$ nm) used to modify the CNTs and form a quenching pair with the QDs ($\lambda_{em} = 525$ nm) (Fig. 2d). The composite with an excess amount of dye shows a lower fluorescence intensity at 525 nm compared with the composite with an excess amount of QDs. It is important to see that even with same amount of QDs, the composite with a higher dye concentration showed a weaker fluorescence at 525 nm from QDs, indicating a fluorescence quenching relationship between the QDs and the coumarin

dye. Thus, in the mCNT/QDs matrix, two mechanisms coexist to reduce fluorescence: (i) FRET between the coumarin dye and the QDs, and (ii) the quenching between CNTs and other fluorescent particles (dye and QDs) via photoinduced electron transfer (PIET) [35,36]. As well, Ishikawa and coworkers observed a drastic decrease in QDs photoluminescence intensity when QDs were conjugated onto SWCNTs (regardless of the size and density) due to a transfer of energy between the QDs and SWCNTs via FRET [37]. Therefore, we propose that the coumarin dye can also serve to weaken the FRET quenching between the

QDs and the CNTs.

Next, the fluorescence characteristics of the as prepared composites were imaged using confocal microscopy. To test the ability of the QDs and the dye molecule from mCNTs to form a FRET pair in the matrix, a composite containing both nanoparticles was prepared and demonstrated limited (or no) fluorescence. First, the fluorescence photos were taken for composites with mCNTs or for composites with QDs. Specifically, the fluorescence for composites containing mCNTs and the composites with QDs were observed separately. By taking fluorescence microscopy images at the middle of the dog bone shaped sample, the composite containing mCNTs exhibits blue fluorescence with low or no green fluorescence (Fig. 2b and c), which matches the results from both the PL measurements and fluorescence spectroscopy above. The epoxy sample with mCNTs exhibits a stronger blue fluorescence (~425 nm) while the green fluorescence (~500 nm) could be barely observed under same exposure and imaging conditions (Figs. 1e and 2a). The composite with QDs exhibited both green and blue fluorescence (Fig. 2e and f) while the green fluorescence was stronger than the blue fluorescence (Figs. 1e and 2a).

Next, composites containing both mCNTs and QDs were prepared and they were either cut with a razor blade or elongated until they broke. First, the composites were cut in the middle with a razor blade (the cutting position and observation area are labeled on the schematic in Fig. 3a and b). In this way, a load was applied only at specific area (i. e., relative to a uniaxial strain experiment) and the composites were subsequently analyzed by fluorescent microscopy. The composites with the mCNTs/QDs pair showed blue and green fluorescence (Fig. 3a and b). This indicates that the mCNTs/QDs quenching pair in the matrix could be utilized as a damage sensor by activating fluorescence via mechanical stimuli and/or physical structure damage. Interestingly, the fluorescence (both green and blue) displayed the highest relative intensity at the damage site and then decreased in intensity towards the center of the sample. In a similar experiment, the effect of the coumarin dye was also probed. A composite containing 0.25 wt% CNTs (i.e., not dye-modified) and 0.005 wt% QDs was prepared and was subjected to cutting via razor blade (Fig. 3a and b left side of the images). This nanocomposite stayed quenched after cutting, which indicated that the quenching of QDs/CNTs was not reversible via mechanical stimuli without the conjugated dye. Metallic surfaces, such as CNTs, have shown to quench the fluorescence from nearby photoexcited dipoles through resonant energy transfer [37]. Herein, the CNTs in the composite provided the metallic surface next to the QDs to quench the fluorescence.

The purpose of this work was to demonstrate mechanically-activated fluorescence in nanocomposites. Ideally, the as-prepared composite would exhibit quenched fluorescence, and then when the composites were subjected to tensile testing they would fluoresce. In related work, Merkoci and coworkers demonstrated that CNTs could be used to irreversibly quench the fluorescence of quantum dots (QDs) [38], which motivated the introduction of the coumarin dye in the work herein. Doorn and coworkers reported that SWCNTs conjugated with a redox-active dye (covalently linked to a specific bio-receptor) caused fluorescence quenching [39]. Furthermore, the fluorescence could be recovered via further interaction between the bio-receptor ligand on the conjugates and target analytes. Also, Jo designed a pH sensor using CNTs by conjugating pyrene to CNTs with a pH-sensitive polysulfonamide linker [40]. In their system, the fluorescence was controlled by the conformation of the polysulfonamide linker: at low pH the polysulfonamide arm collapsed and the pyrene was brought towards the CNTs in order to quench the fluorescence, whereas at higher values of pH the pyrene dye was far enough away from the CNTs in order to fluoresce. In the work herein, the cured nanocomposites were subjected to tensile testing until failure and analyzed using fluorescent microscopy. Fig. 3c and d shows a representative sample, wherein composites containing of mCNTs and QDs were broken using tensile testing and then analyzed (the approximate region imaged is labeled in the schematic shown alongside Fig. 3c and d). The fluorescence microscopy photos of the pre-tensile precursors (Fig. 3c and d, left) show a significantly lower fluorescence intensity than the images of the samples after tensile testing (Fig. 3c and d, right). The mechanically triggered fluorescence confirms the original intention of design: the mCNTs/QDs pair exhibit stimuli-responsive behavior. The quenching phenomenon of composites with mCNTs and QDs could be because of both FRET quenching between coumarin dye and QDs, and the electron-hole energy transfer between the CNTs and QDs.

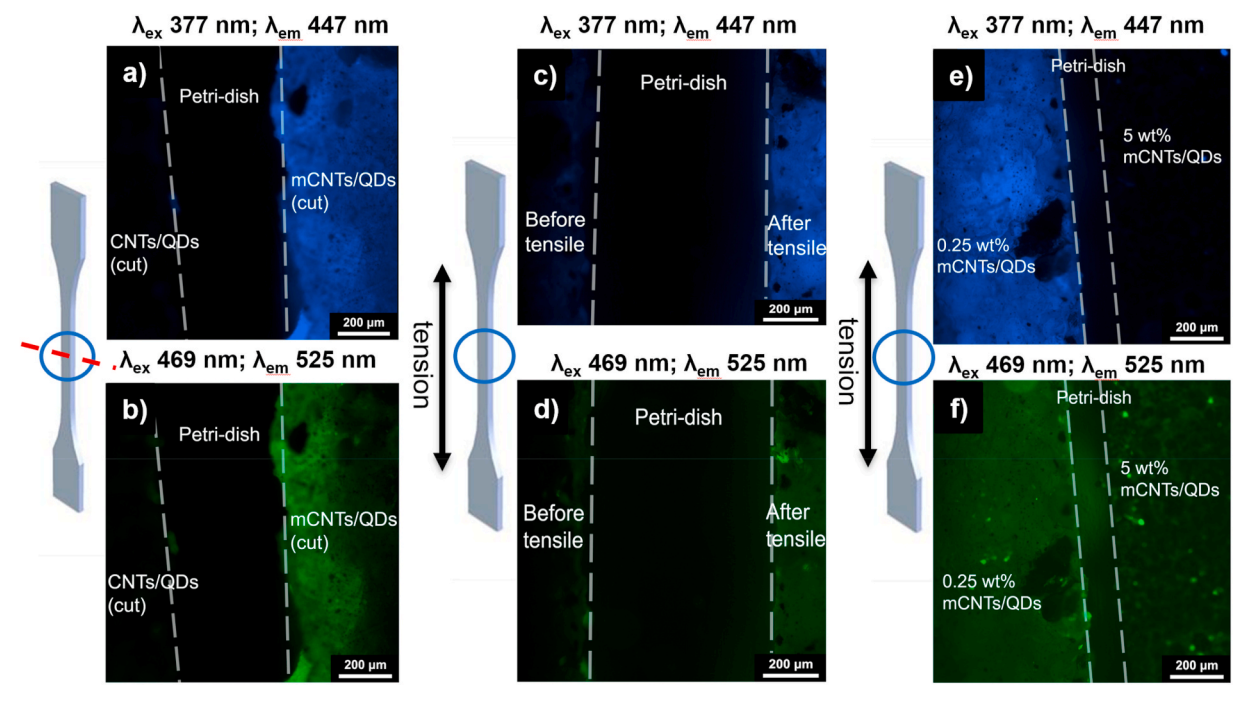


Fig. 3. Fluorescence micrographs of (a,b) composites containing QDs and either CNTs (bare) or mCNTs (modified with the coumarin dye) after cutting with a razor blade (c,d) composites containing mCNTs and QDs before and after tension experiments, QDs concentration: 0.005 wt%, mCNTs concentration: 0.25 wt%. (e,f) composites containing 0.005 wt% QDs and either 0.25 wt% or 5 wt% mCNTs before and after tension experiments. Tension: 0.5 mm/min until break.

In the mCNTs/QDs epoxy matrix herein, the hydrogen bonding and/ or dipole interactions between the carboxylic acid group on the CNTs and the ether and amine functional groups on the Jeffamine curing agents result in good dispersion of the CNTs in the epoxy matrix. Therefore, the load from mechanical stimuli (via uniaxial strain or the dissection process) transmitted along the epoxy back bone towards the CNTs would form CNT bridges. As a result, the distance between mCNTs and QDs in the 'damaged' composite would increase, which weakens the quenching effect between dye-QDs, CNTs-QDs, and mCNTs-QDs. Subsequently, as the quenching efficiency between the pair decreases, the fluorescence properties reemerge as both green and blue fluorescence. However, the matrix with CNTs/QDs (i.e., no coumarin dye) stayed quenched even after mechanical stimuli. This could be because the electron transfer efficiency from the QDs to the CNTs by the photoinduced intramolecular electron transfer (PIET) quenching pathway is too strong to overcome.

A potential concern was that the mechanoresponsive phenomenon of the composite containing mCNTs/QDs would be sensitive to the nanoparticle loading and the stoichiometry of QDs:mCNTs. Thus, the concentration of mCNTs was raised as high as 5 wt% while the QDs concentration stayed the same at 0.005 wt%. After tensile testing, no significant activation of fluorescence was observed (Fig. 3e and f). This is further proof that the coumarin dye on the surface of mCNTs prevented the fluorescent quenching of QDs to a certain degree. By increasing the concentration of mCNTs in the matrix, the average distance between QDs and mCNTs decreased, which likely increased CNT-QD interaction (i.e., the irreversible quenching) as well as reduced the probability of an increased CNT-QD distance after the application of a mechanical stimulus. In either case, the matrix remained quenched after the mechanical stimuli. This result also confirmed the mechanism of fluorescence is not dominated by FRET. At higher mCNTs levels, the chance of energy transfer to the potential FRET acceptor, which is the QD in this system, should result in higher fluorescence intensity by the QDs. However, the sample with 5 wt% mCNTs did not display stronger fluorescence (blue or green) when compared with the sample containing only 0.25 wt% mCNTs.

Fluorescence mapping taken with photoluminescence (PL) spectroscopy provided additional details of the fluorescence intensity distribution within the epoxy matrix containing mCNTs/QDs and subjected to tensile testing (Figure S1). Fluorescence spectra were taken at both the sample center (red) and the sample edge close to the clamp (black). As observed, the fluorescence at 450 nm and 525 nm from the center showed almost double the intensity compared with the spectrum of the sample edge, indicating that the sample center experienced larger spatial displacement resulting in a stronger fluorescence intensity. Interestingly, the blue fluorescence (450 nm) at the sample edge was stronger than the green fluorescence (525 nm).

For samples with 0.25 wt% mCNTs and 0.005 wt% QDs, the mCNTs and QDs dispersion within the epoxy before and after tension was investigated with TEM (Fig. 4). Before the tension was applied, the mCNTs and QDs are well dispersed within the polymer matrix composite system (Fig. 4a,b,c); no significant aggregation was observed and the QDs were seen mainly in areas close to the mCNTs. This could be because of a relatively stronger interaction between the mCNTs and the QDs compared to the interaction between the mCNTs and the matrix and the QDs and the matrix. The mCNTs were seen as elongated cylinders within the sample before tension was applied. However, the morphology of the mCNTs changed dramatically after tension was applied to the sample (Fig. 4d,e,f). It has been shown that surface modifications can reduce the tensile strength and modulus of carbon nanotubes [41]; thus, the acid modification to the carbon nanotubes together with the dye conjugation could possibly weaken the carbon nanotubes. Moreover, residual acid groups on the CNTs could react with the Jeffamine hardener during the resin curing, which would make the CNTs more susceptible to mechanical failure under an applied load.

The TEM images also provided information about the average distance between the mCNTs and QDs within the composite. The TEM images of the composites before tension was applied indicate that the QDs-mCNTs distance was less than 20–50 nm. The sections for TEM were cryogenically microtomed at a thickness of 80 nm; thus, we cannot

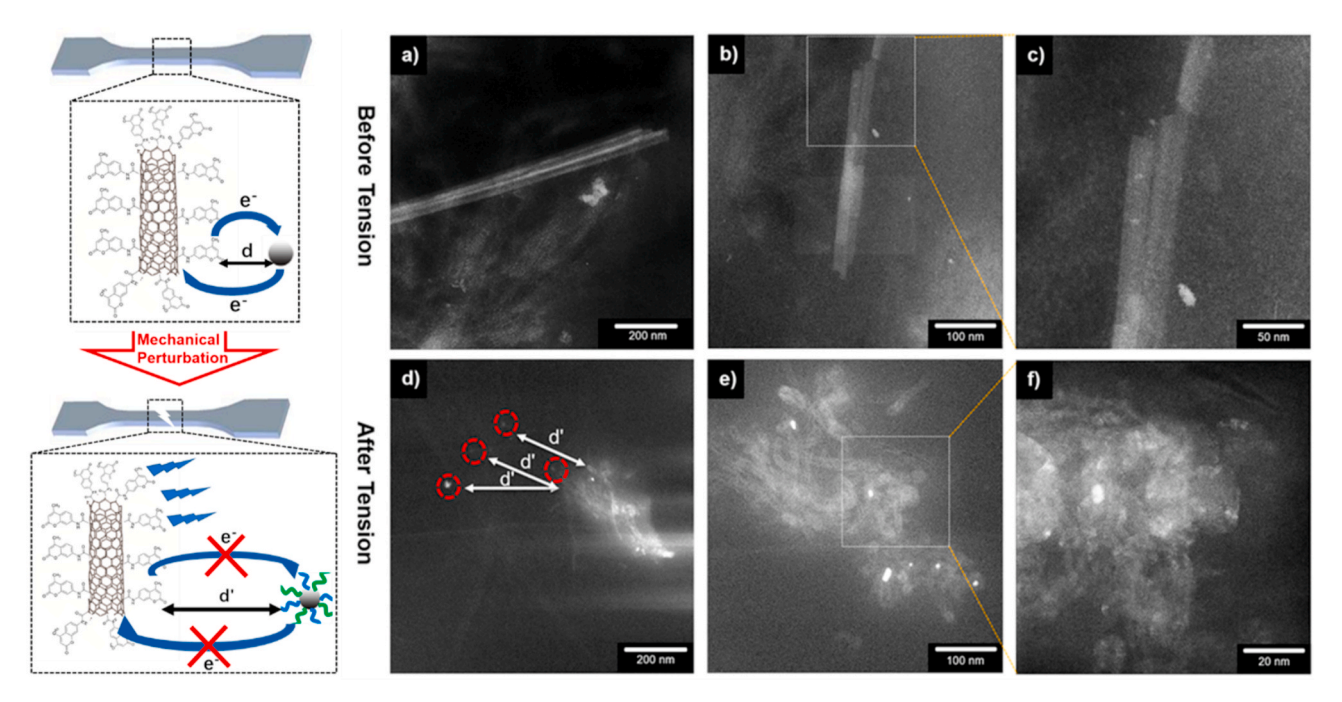


Fig. 4. Transmission electron micrographs of composites containing mCNTs and QDs: (a–c) before tension was applied, and (d–f) after tension was applied. (a) Before tension was applied, the QDs were observed on the surface of mCNTs as brighter dots. (b) An intermediate magnification to a and c before tension was applied showing a relatively small mCNT-QD spacing. (c) A closer view of the selected area from b. (d) After tension was applied, the QDs were observed on the surface of mCNTs as brighter dots. (e) An intermediate magnification after tension was applied showing an increase in the mCNT-QD spacing caused by the strain. (f) A closer view of the selected area from e. QDs concentration: 0.005 wt%, mCNTs concentration: 0.25 wt%. Tension: 0.5 mm/min until break.

overrule the possibility of the QDs being projected onto the mCNTs. However, the QDs and CNTs appear close together. Whereas, after tension was applied to the composites the distance between the QDs and mCNTs appears to increase. The QDs appeared to be separated from mCNTs and the distance between the two additives was \sim 250 nm. This result further confirms that the mechanically-activated fluorescence is related to the distance between the fluorescent additives. The hypothesized mechanism of fluorescence quenching is that electrons are transferred between the mCNTs and the QDs when the pair are at a close distance. After mechanical stimulus is applied to the nanocomposite (whether tension or cutting), the average distance between the mCNTs and QDs increased, which dramatically reduced the efficiency of electron transfer between mCNTs and QDs. Therefore, the excited electrons from the coumarin dye on mCNTs as well as the QDs stay in their original system, which manifested as fluorescence in the samples after the mechanical stimulus was applied. The previous PL fluorescence test (Figure S1), which showed fluorescence after tensile testing at the same wavelength as the original mCNTs and QDs, provides further proof that the fluorescence after application of the mechanical stimulus comes from the coumarin dve on mCNTs and the QDs rather than some other

Next, the sensitivity of the damage sensor was tested by controlling the strain applied to the sample, rather than straining the sample until complete failure. Fluorescence microscopy was used alongside the tensile tests to evaluate the fluorescence in the composites at strain values of 0, 2.5, 5, 7.5, 10, and 15%. The representative fluorescence intensities for the selected strain values for the mCNTs/QDs epoxy nanocomposites can be seen in Fig. 5a and b. Representative fluorescence micrographs can be seen in Figure S2. The fluorescence intensity is plotted against strain for both blue and green fluorescence in the mCNTs/QDs composites. There is an overall increase in the fluorescence with an increase of the strain applied; however, there is no statistically significant difference between the samples imaged at 0, 2.5, and 5% strain. However, at 7.5% strain the fluorescence intensity increases relative to the baseline, and subsequent increases in strain produce further statistically significant differences in fluorescence intensity. These measurable differences would be required for damage detection. Of note is that both the blue and green fluorescence intensity curves exhibit a similar trend.

The tensile testing performance of the various composites is shown in Fig. 5c. The properties of the neat matrix (without any nanoparticle added) are compared to the composites containing 1) the combination of the QDs and variable mCNTs concentrations (QDs concentration is 0.005 wt%) and 2) the QDs. As the concentration of mCNTs increased, the Young's modulus and the strain at break increased, and the composite with 0.75 wt% mCNTs displayed the best mechanical properties based on Young's modulus. The composite with 1 wt% mCNTs displayed the highest strain at break; however, the Young's modulus was lower

than the sample with 0.75 wt% mCNTs. Further addition of mCNTs (e.g., 2 wt% mCNTs) degraded the mechanical properties even more. The decrease in mechanical properties could be due to the mCNTs inhibiting the curing process or aggregating at the higher volume fractions; both effects would limit the mechanical properties of the composite. The composite with QDs only, on the other hand, showed slightly worse mechanical properties compared with the neat matrix. This suggests some sort of plasticization or free volume effect or an inhibition to the curing process.

CNTs are perhaps today's most popular additive, with the first report highlighting the dispersion and alignment of CNTs in a composite in 1994 [42]. CNTs modulate the properties of composites in a variety of ways, most commonly by enhancing the mechanical properties and the electrical conductivity [43]. Numerous studies have investigated the impact that CNTs have on the thermomechanical properties of elastomeric and glassy composites [33,44,45]. Several studies have highlighted the importance of overcoming CNT agglomeration; for example, grafting silane molecules onto the CNTs significantly improved the dispersion in a composite comprised of BADGE and m-phenylenediamine [46]. The enhanced CNT dispersion improved the mechanical performance because the propagating cracks in the matrix were forced to bypass the CNTs, which resulted in long, tortuous paths. Similarly, CNT bridges (i.e., a CNT spanning across a crack) can restrict crack formation and mechanical failure while improving the overall mechanical strength, because the force needed to break CNTs was greater than that needed for pullout of CNTs. The pull-out mechanism is known as the most significant contribution to enhancing the mechanical properties of epoxy matrix nanocomposites [47]. In the context of this work, the combination of nanoparticle-nanoparticle interactions (to modulate fluorescence) and nanoparticle-matrix interactions (to modulate thermomechanical properties) can be manipulated separately to decouple multifunctional characteristics from composite failure diagnosis and sensitivity.

4. Conclusions

Using a combination of nanoparticles that form a fluorescence quenching pair successfully enabled mechanoresponsive behavior in the composite. The addition of the QDs decreases the Young's modulus and the stress at break while increasing the strain at break slightly, the addition of the mCNTs increased each of these characteristics. QDs/mCNT composites display fluorescence quenching, while fluorescence can be activated via mechanical strain and/or physical damage to the composite. However, QDs/CNTs composites (with no dye) displayed irreversible quenching, indicating that the dye was an important buffer between the QDs and the CNTs. Finally, 7.5% of mechanical strain will activate the fluorescence in the polymer matrix composites. Overall,

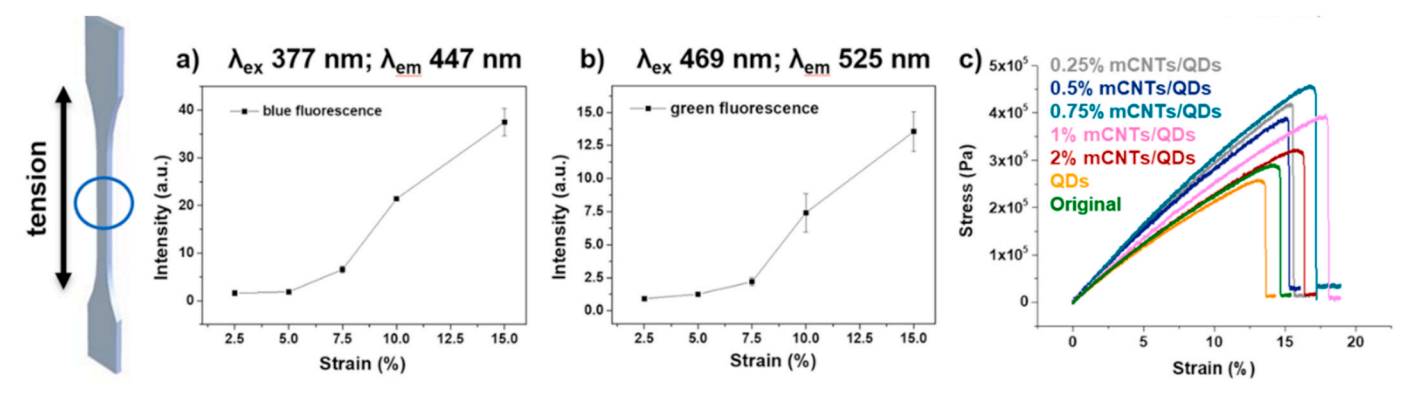


Fig. 5. The panels show the fluorescence intensity for mCNTs/QDs composites at varying applied strain. (a) excitation wavelength: 377 nm and emission wavelength: 447 nm; (b) excitation wavelength: 469 nm and emission wavelength: 525 nm. QDs concentration: 0.005 wt%, mCNTs concentration: 0.25 wt%. (c) Tensile analysis of composites containing different concentrations of mCNTs and QDs.

these results offer a new route for composite failure diagnosis that is decoupled from complicated synthesis schemes and without interfering with the multifunctional nature of nanoparticle-modified composites.

Declaration of competing interest

The authors declare that they have no known competing financial interests or personal relationships that could have appeared to influence the work reported in this paper.

Acknowledgements

This work was financially supported in part by the Army Research Office (W911NF-19-1-0132, W911NF-18-1-0412, W911NF-16-1-0271, W911NF-15-1-0353), and ASU's DoD Seed Grant. S.T acknowledges support from DOE-SC0020653, NSF DMR 1552220, NSF DMR 1904716, and NSF CMMI 1933214.

Appendix A. Supplementary data

Supplementary data to this article can be found online at https://doi.org/10.1016/j.polymer.2020.123275.

References

- [1] M.M. Caruso, D.A. Davis, Q. Shen, S.A. Odom, N.R. Sottos, S.R. White, J.S. Moore, Mechanically-induced chemical changes in polymeric materials, Chem. Rev. 109 (11) (2009) 5755–5798.
- [2] H. Staudinger, E.O. Leupold, Über Isopren und Kautschuk, 18. Mitteil.: viscositäts-Untersuchungen an Balata, Ber. Dtsch. Chem. Ges. 63 (3) (1930) 730–733.
- [3] H. Staudinger, H.F. Bondy, Über Isopren und Kautschuk, 19. Mitteil.: Über die Molekülgröße des Kautschuks und der Balata, Ber. Dtsch. Chem. Ges. 63 (3) (1930) 734–736.
- [4] J. Sohma, Mechanochemistry of polymers, Prog. Polym. Sci. 14 (4) (1989) 451–596.
- [5] J.M. Lenhardt, M.T. Ong, R. Choe, C.R. Evenhuis, T.J. Martinez, S.L. Craig, Trapping a diradical transition state by mechanochemical polymer extension, Science 329 (5995) (2010) 1057–1060.
- [6] C.R. Hickenboth, J.S. Moore, S.R. White, N.R. Sottos, J. Baudry, S.R. Wilson, Biasing reaction pathways with mechanical force, Nature 446 (7134) (2007) 423–427
- [7] J.Z. Du, X.J. Du, C.Q. Mao, J. Wang, Tailor-made dual pH-sensitive polymer-doxorubicin nanoparticles for efficient anticancer drug delivery, J. Am. Chem. Soc. 133 (44) (2011) 17560–17563.
- [8] D.A. Davis, A. Hamilton, J.L. Yang, L.D. Cremar, D. Van Gough, S.L. Potisek, M. T. Ong, P.V. Braun, T.J. Martinez, S.R. White, J.S. Moore, N.R. Sottos, Force-induced activation of covalent bonds in mechanoresponsive polymeric materials, Nature 459 (7243) (2009) 68–72.
- [9] C.E. Diesendruck, B.D. Steinberg, N. Sugai, M.N. Silberstein, N.R. Sottos, S. R. White, P.V. Braun, J.S. Moore, Proton-coupled mechanochemical transduction: a mechanogenerated add, J. Am. Chem. Soc. 134 (30) (2012) 12446–12449.
- [10] M.B. Larsen, A.J. Boydston, Flex-Activated" mechanophores: using polymer mechanochemistry to direct bond bending activation, J. Am. Chem. Soc. 135 (22) (2013) 8189–8192.
- [11] T. Shiraki, C.E. Diesendruck, J.S. Moore, The mechanochemical production of phenyl cations through heterolytic bond scission, Faraday Discuss 170 (2014) 385–394.
- [12] Y. Sagara, S. Yamane, M. Mitani, C. Weder, T. Kato, Mechanoresponsive luminescent molecular assemblies: an emerging class of materials, Adv. Mater. 28 (6) (2016) 1073–1095.
- [13] A. Pucci, R. Bizzarri, G. Ruggeri, Polymer composites with smart optical properties, Soft Matter 7 (8) (2011) 3689–3700.
- [14] J. Luo, L.Y. Li, Y. Song, J. Pei, A piezochromic luminescent complex: mechanical force induced patterning with a high contrast ratio, Chemistry—A European Journal 17 (38) (2011) 10515–10519.
- [15] H. Naito, Y. Morisaki, Y. Chujo, o-Carborane-based anthracene: a variety of emission behaviors, Angew. Chem. Int. Ed. 54 (17) (2015) 5084–5087.
- [16] Z. Ma, Z. Wang, Z. Xu, X. Jia, Y. Wei, Controllable multicolor switching of oligopeptide-based mechanochromic molecules: from gel phase to solid powder, J. Mater. Chem. C 3 (14) (2015) 3399–3405.
- [17] Z. Ma, M. Teng, Z. Wang, S. Yang, X. Jia, Mechanically induced multicolor switching based on a single organic molecule, Angew. Chem. Int. Ed. 52 (47) (2013) 12268–12272.
- [18] M.S. Kwon, J. Gierschner, S.J. Yoon, S.Y. Park, Unique piezochromic fluorescence behavior of dicyanodistyrylbenzene based donor-acceptor-donor triad:

- mechanically controlled photo-induced electron transfer (eT) in molecular assemblies, Adv. Mater. 24 (40) (2012) 5487–5492.
- [19] S.-J. Yoon, J.W. Chung, J. Gierschner, K.S. Kim, M.-G. Choi, D. Kim, S.Y. Park, Multistimuli two-color luminescence switching via different slip-stacking of highly fluorescent molecular sheets, J. Am. Chem. Soc. 132 (39) (2010) 13675–13683.
- [20] H.J. Kim, D.R. Whang, J. Gierschner, C.H. Lee, S.Y. Park, High-Contrast red-green-blue tricolor fluorescence switching in bicomponent molecular film, Angew. Chem. Int. Ed. 54 (14) (2015) 4330–4333.
- [21] S.J. Choi, J. Kuwabara, Y. Nishimura, T. Arai, T. Kanbara, Two-step changes in luminescence color of Pt (II) complex bearing an amide moiety by mechano-and vapochromism, Chem. Lett. 41 (1) (2012) 65–67.
- [22] C. Lowe, C. Weder, Oligo(p-phenylene vinylene) excimers as molecular probes: deformation-induced color changes in photoluminescent polymer blends, Adv. Mater. 14 (22) (2002) 1625–1629.
- [23] J.D. Luo, Z.L. Xie, J.W.Y. Lam, L. Cheng, H.Y. Chen, C.F. Qiu, H.S. Kwok, X. W. Zhan, Y.Q. Liu, D.B. Zhu, B.Z. Tang, Aggregation-induced emission of 1-methyl-1,2,3,4,5-pentaphenylsilole, Chem. Commun. (18) (2001) 1740–1741.
- [24] C. Weder, MECHANOCHEMISTRY Polymers react to stress, Nature 459 (7243) (2009) 45–46.
- [25] G.R. Gossweiler, G.B. Hewage, G. Soriano, Q.M. Wang, G.W. Welshofer, X.H. Zhao, S.L. Craig, Mechanochemical activation of covalent bonds in polymers with full and repeatable macroscopic shape recovery, ACS Macro Lett. 3 (3) (2014) 216–219.
- [26] J.W. Woodcock, R. Beams, C.S. Davis, N. Chen, S.J. Stranick, D.U. Shah, F. Vollrath, J.W. Gilman, Observation of interfacial damage in a silk-epoxy composite, using a simple mechanoresponsive fluorescent probe, Advanced Materials Interfaces 4 (10) (2017) 1601018.
- [27] S.K. Kumar, B.C. Benicewicz, R.A. Vaia, K.I. Winey, 50th anniversary perspective: are polymer nanocomposites practical for applications? Macromolecules 50 (3) (2017) 714–731.
- [28] A.J. Crosby, J.Y. Lee, Polymer nanocomposites: the "nano" effect on mechanical properties, Polym. Rev. 47 (2) (2007) 217–229.
- [29] J.W.C. Pang, I.P. Bond, A hollow fibre reinforced polymer composite encompassing self-healing and enhanced damage visibility, Compos. Sci. Technol. 65 (11–12) (2005) 1791–1799.
- [30] K. Makyla, C. Muller, S. Lorcher, T. Winkler, M.G. Nussbaumer, M. Eder, N. Bruns, Fluorescent protein senses and reports mechanical damage in glass-fiber-reinforced polymer composites, Adv. Mater. 25 (19) (2013) 2701–2706.
- [31] B.X. Du, M. Xiao, J.W. Zhang, Effect of thermal conductivity on tracking failure of epoxy/BN composite under pulse strength, Ieee T Dielect El In 20 (1) (2013) 296–302.
- [32] D. Wentzel, S. Millers, I. Sevostianov, Dependence of the electrical conductivity of graphene reinforced epoxy resin on the stress level, Int. J. Eng. Sci. 120 (2017) 63–70.
- [33] M. Wang, E. Dheressa, K.A. Brown, M.D. Green, Effect of crosslinker length and architecture on the thermomechanical properties of CNT-loaded elastomeric polymer matrix composites, Macromol. Rapid Commun. 39 (14) (2018).
- [34] J.C. Sheehan, G.P. Hess, A new method of forming peptide bonds, J. Am. Chem. Soc. 77 (4) (1955) 1067–1068.
- [35] B.N.J. Persson, N.D. Lang, Electron-hole-pair quenching of excited-states near a metal, Phys. Rev. B 26 (10) (1982) 5409–5415.
- [36] W.L. Barnes, Fluorescence near interfaces: the role of photonic mode density, J. Mod. Optic. 45 (4) (1998) 661–699.
- [37] V. Biju, T. Itoh, Y. Baba, M. Ishikawa, Quenching of photoluminescence in conjugates of quantum dots and single-walled carbon nanotube, J. Phys. Chem. B 110 (51) (2006) 26068–26074.
- [38] E. Morales-Narvaez, B. Perez-Lopez, L.B. Pires, A. Merkoci, Simple Forster resonance energy transfer evidence for the ultrahigh quantum dot quenching efficiency by graphene oxide compared to other carbon structures, Carbon 50 (8) (2012) 2987–2993.
- [39] B.C. Satishkumar, L.O. Brown, Y. Gao, C.C. Wang, H.L. Wang, S.K. Doorn, Reversible fluorescence quenching in carbon nanotubes for biomolecular sensing, Nat. Nanotechnol. 2 (9) (2007) 560–564.
- [40] E.S. Cho, S.W. Hong, W.H. Jo, A new pH sensor using the fluorescence quenching of carbon nanotubes, Macromol. Rapid Commun. 29 (22) (2008) 1798–1803.
- [41] K. Naito, J.-M. Yang, Y. Inoue, H. Fukuda, The effect of surface modification with carbon nanotubes upon the tensile strength and Weibull modulus of carbon fibers, J. Mater. Sci. 47 (23) (2012) 8044–8051.
- [42] P.M. Ajayan, O. Stephan, C. Colliex, D. Trauth, Aligned carbon nanotube Arrays formed by cutting a polymer resin-nanotube composite, Science 265 (5176) (1994) 1212–1214.
- [43] Y. Liu, S. Kumar, Polymer/carbon nanotube nano composite fibers—A review, ACS Appl. Mater. Interfaces 6 (9) (2014) 6069–6087.
- [44] P.-C. Ma, N.A. Siddiqui, G. Marom, J.-K. Kim, Dispersion and functionalization of carbon nanotubes for polymer-based nanocomposites: a review, Compos. Appl. Sci. Manuf. 41 (10) (2010) 1345–1367.
- [45] K.I. Winey, R.A. Vaia, Polymer nanocomposites, MRS Bull. 32 (4) (2007) 314-322.
- [46] P.C. Ma, J.K. Kim, B.Z. Tang, Effects of silane functionalization on the properties of carbon nanotube/epoxy nanocomposites, Compos. Sci. Technol. 67 (14) (2007) 2965–2972.
- [47] J.K. Kim, Y.W. Mai, High-strength, high fracture-toughness fiber composites with interface control - a review, Compos. Sci. Technol. 41 (4) (1991) 333–378.